Acta Cryst. (1975). A31, 201

Anharmonic Thermal Vibrations in Wurtzite Structures

BY SYLVIA L. MAIR* AND ZWI BARNEA

School of Physics, University of Melbourne, Parkville, Victoria, Australia, 3052

(*Received* 5 *August* 1974; *accepted* 5 *September* 1974)

The general form of the effective one-particle potential has been derived up to cubic terms for an atom undergoing anharmonic thermal vibration in a wurtzite-type crystal. The resulting potential suggests a mechanism for the primary pyroelectricity observed in these structures. The deviation of the structural parameters u in the various wurtzite structures from their predicted values, is shown to be closely related to the pyro-electric effect, and can also be attributed to anharmonicity. The effects of anharmonicity on the elastic scattering of X-rays and neutrons have been investigated. It is shown that the u parameter in the conventional expression for the Bragg intensities implicitly contains first-order anharmonic effects, but that a modified form of the intensity expression is necessary to account for higher-order anharmonic effects.

Introduction

Anharmonic thermal vibrations have been investigated in several cubic substances through the use of an effective one-particle potential (Dawson & Willis, 1967; Willis, 1969). Their effect on the elastic X-ray or neutron scattering is particularly marked when some of the atoms occupy sites which are not centres of inversion symmetry, since this allows the one-particle potential to have non-zero antisymmetric terms. It may be said in general that the lower the symmetry of the structure, the more varied the anharmonic effects are likely to become. Thus if a crystal in a non-cubic symmetry group contains non-centrosymmetric atomic sites, the equilibrium positions of the atoms on those sites will not in general coincide with their mean positions.

The majority of crystal structures belong to non-cubic symmetry groups. As the symmetry is lowered there is a corresponding increase in the number of independent parameters necessary to define the effective one-particle potential. The wurtzite structure, with hexagonal symmetry (see Fig. 1), and hence a relatively small number of independent parameters, offers a particularly interesting and amenable problem. This structure is closely related to the cubic zincblende structure, the atoms of which have been shown to exhibit anharmonic motion equally along the four tetrahedrally oriented antibonding directions (Cooper, Rouse & Fuess, 1973). We expect a similar type of motion to occur in the wurtzite compounds, but the amplitude along the c axis will not be constrained to equal that along the three other antibonding directions.

The procedure we shall follow is to derive the effective one-particle potential for the wurtzite structure from the atomic point-group symmetry. We shall then examine the effect of the atomic motion allowed by this potential upon the structural parameter u and the pyro-electric effect. Finally, using the generalized structure-factor formalism of Dawson (1967), the intensities of elastic X-ray or neutron scattering will be obtained and the effect of anharmonicity on these intensities discussed.

* Present address: Division of Chemical Physics, CSIRO, P. O. Box 160, Clayton, Victoria, Australia, 3168.

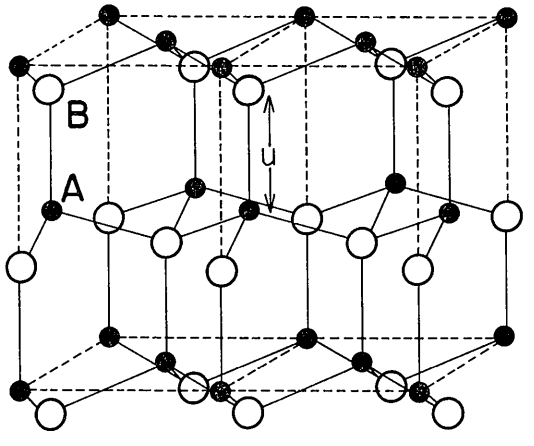

Fig. 1. Schematic representation of the wurtzite structure.

The effective one-particle potential

In describing the potential in which an atom vibrates it is convenient to assume that there is no coupling between the atomic vibrations. The vibration of a particular atom is then influenced only by the other atoms at their rest positions. Under this condition the general form for the potential of the μth atom in the crystal is

$$V^{\mu} = V_0^{\mu} + V_{ij}^{\mu} x_i x_j + V_{ijk}^{\mu} x_i x_j x_k \,, \qquad (1)$$

where x_i, x_j and x_k are the ith, jth and kth coordinates along the hexagonal axes a_1, a_2 and c, of the atom's displacement from its rest position. In equation (1) the summation convention for repeated indices has been assumed and terms of order higher than cubic in the

x_i have been ignored. The superscript μ will be omitted in some equations below.

The point-group symmetry for the sites of both atomic species is $3m$. By applying the conditions that the tensors V_{ij}, V_{ijk} are invariant under the operations corresponding to this point-group symmetry, the expression for V simplifies to the form:

$$V = V_0 + V_2 + V_3 \tag{2}$$

where

$$V_2 = \frac{\alpha_1}{2}(x_1^2 - x_1x_2 + x_2^2) + \frac{\alpha_3}{2}x_3^2 \tag{3}$$

and

$$V_3 = \beta_1(x_1x_2^2 - x_2^2x_1) + \beta_2(x_1^2 - x_1x_2 + x_2^2)x_3 + \beta_3x_3^3 . \tag{4}$$

The quadratic part V_2 describes the well-known harmonic motion, with the α_i related to the harmonic Debye–Waller factors by equations (16) and (17). Represented in polar coordinates, it forms an ellipsoid of revolution about the c axis.

The three cubic terms, with coefficients, β_i, are also most clearly pictured through polar diagrams. Fig. 2 represents the first term of equation (4). It consists of three positive and three negative lobes, alternately radiating out from the c axis in directions at $\pi/3$ intervals in the $c=0$ plane. The second and third terms of equations (4) are volumes of revolution about the c axis. They are shown in Figs. 3 and 4 respectively. It should be noted that the signs of the lobes for a particular term can be interchanged by changing the sign of the relevant β coefficient. Since the most stable configuration is that for which the potential is a minimum, the negative lobe should indicate the preferred directions of motion of the atom.

Each atom is surrounded by four holes, in tetrahedral coordination. Three of these are equivalent octahedral sites and the fourth, centred on the c axis, is a tetrahedral site. It is in the directions of these four holes that one would expect the negative lobes of the potential to lie. This can be ensured by minimization of V_3, expressed in polar coordinates in the directions of the three octahedral holes. The equations to be satisfied are:

$$\left.\frac{\partial V_3}{\partial \varphi}\right|_h = 0 \tag{5}$$

$$\left.\frac{\partial^2 V_3}{\partial \varphi^2}\right|_h > 0 \quad . \tag{6}$$

Here, φ is the angle between **x** and the c axis, and the subscript h indicates that the derivatives must be evaluated in the direction of an octahedral hole.

For an ideal wurtzite structure we have $c/a = \sqrt{8/3}$ and the positional parameter u, giving the distance between nearest neighbours along the c axis, is 3/8. In this case equations (5) and (6) give the following relationship:

$$\tfrac{8}{9}|\beta_1| - |\beta_2| + \tfrac{3}{16}|\beta_3| = 0 . \tag{7}$$

With the signs of β_1, β_2 and β_3 chosen according to Table 1, and with equations (5) and (6) satisfied, the three cubic terms combine to form the potential V_3, whose main features are four negative lobes directed towards the holes and four corresponding positive lobes lying in the opposite directions. The polar diagram in the plane containing the c axis and the centre of one of the octahedral holes is shown in Fig. 5 for the case of a cation.

It is difficult to predict the size of the lobe along the c axis relative to the other lobes. It will depend on the

Table 1. *Signs of coefficients of cubic potential terms*

	Cations (A)	Anions (B)
β_1	+	+
β_2	−	+
β_3	+	−

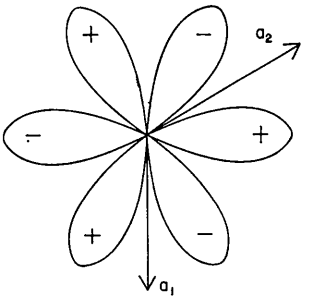

Fig. 2. Polar diagram representing the term $\beta_1(x_1x_2^2 - x_2^2x_1)$ of V_3, in the plane $c=0$.

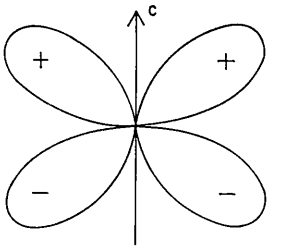

Fig. 3. Polar diagram representing the term $\beta_2(x_1^2 - x_1x_2 + x_2^2)$ of V_3, for all planes containing the c axis.

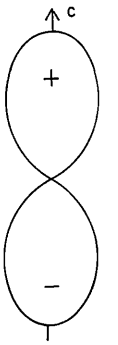

Fig. 4. Polar diagram representing the term $\beta_3x_3^3$ of V_3, for all planes containing the c axis.

relative strength of the bond along the c axis compared with that of the other three bonds. In Fig. 5, the ratios $|\beta_3|/|\beta_2|$ and $|\beta_1|/|\beta_2|$ have been chosen as 64/45 and 33/40 respectively. These values are based solely on the relative dimensions of the octahedral and tetrahedral holes, located in the four antibonding directions, under the somewhat arbitrary assumption that

$$\frac{V_3(\text{oct})}{V_3(\text{tet})} = \frac{d^2(\text{oct})}{d^2(\text{tet})} \quad . \tag{8}$$

In this relation, V_3(oct) is the cubic potential in the direction of an octahedral hole, V_3(tet) is its value in the direction of the tetrahedral hole, d(oct) and d(tet) are the distances from the atomic rest position to the centres of the respective holes. The relationship serves merely as a device to obtain a possible shape for the potential function, and is likely to be of greater validity for covalent compounds, where steric effects would be expected to dominate.

Anharmonic effects and the *u* parameter

If motion towards one type of hole adjacent to an atomic site is preferred over motion towards the other type, it follows that the mean (time-averaged) position of the atom will not correspond to its equilibrium position. One position will be translated along the c axis with respect to the other. In conventional structure determinations, the atom is constrained to vibrate in a harmonic potential and this results in the determination of the mean positions of the atoms. Thus the parameter u defining the nearest-neighbour distance along the c axis as a fraction of c, is in general, when obtained by traditional methods, a distance between mean positions.

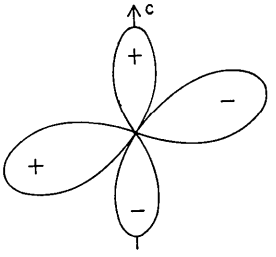

Fig. 5. Polar diagram representing V_3 for a cation in an ideal wurtzite structure in the plane containing the c axis and the centre of one of the octahedral holes.

In the ideal hexagonal close-packed structure the lattice-parameter ratio, c/a, has the value $\sqrt{8/3}$ and the u parameter is 3/8. If c/a is different from this ideal value, the lattice is composed of distorted tetrahedra. Keffer & Portis (1957) have suggested two expressions for the corresponding u parameter, depending upon whether (*a*) bond stretching or (*b*) bond bending dominates as a result of the change in c/a. Both expressions tend to underestimate the observed u values, but that for case (*a*),

$$u' = \tfrac{1}{3}\left(\frac{a}{c}\right)^2 + \tfrac{1}{4} \tag{9}$$

is always the closer.

Table 2 lists experimentally observed u parameters for wurtzite compounds, in order of increasing c/a. The values u' predicted by equation (9) and the differences between u and u' are also shown. In all cases except those of AgI and NH_4F the observed values are larger than the predicted ones. For NH_4F the predicted value is calculated under the assumption that c/a is the same at −196 °C as at room temperature. This is probably justified, since in the case of BeO c/a changes by only 0·2% for a 900 °C change in temperature. The observed u parameter for NH_4F at −196 °C is then the same as that predicted by equation (9). We are therefore led to believe that the difference between observed and predicted u values at the higher temperatures is due to anharmonic motion of the atoms, with vibration along the c axis being slightly preferred over vibration in the other three antibonding directions. For the case of NH_4F at −196 °C, the anharmonic component of the motion has been damped so much as to become negligible.

The validity of this explanation may readily be tested by refinement of the intensity data with provision made

Table 2. *Observed and calculated values of the structural parameter u in order of increasing c/a*

Compound	c/a	u (observed value)	u' [as for equation (9)]	$u-u'$
AlN	1·600	0·385[1]	0·380	0·005
ZnO	1·602	*0·3826 (0·0007)[2]	0·3799	0·0027 (0·0007)
NH_4F	1·614	*0·3780 (0·0004)[3] (at −196 °C)	0·3780	0·0000 (0·0004)
BeO	1·620	*0·3795 (0·0010)[4] (at 900 °C)	0·3770	0·0026 (0·0010)
	1·623	0·3786 (0·0005)[5]	0·3765	0·0021 (0·0005)
CdS	1·623	0·3775 (0·0003)[6]	0·3765	0·0010 (0·0003)
CdSe	1·631	0·3767 (0·0002)[7]	0·3753	0·0014 (0·0002)
AgI	1·635	0·3747 (0·0015)[8]	0·3747	0·0000 (0·0015)

References: 1. Jeffrey, Parry & Mozzi (1956); 2. Sabine & Hogg (1969); 3. Adrian & Feil (1969); 4. Pryor & Sabine (1964); 5. Smith, Newkirk & Kahn (1964); 6. J. Castles. (private communication); 7. Barnea (1973); 8. Burley (1963).

* These parameters are from neutron rather than X-ray measurements. All parameters are measured at room temperature unless otherwise indicated.

for anharmonicity. Distances between equilibrium, rather than mean positions of the atoms would then be obtained, and u should equal u' for all of the wurtzite compounds.

Inspection of Table 2 reveals that there is a consistent decrease in the difference $u-u'$ as c/a increases towards the ideal value of 1·633, for an undistorted hexagonal close-packed lattice. In the case of AgI, with c/a very close to this ideal, the difference is zero. Of course, we expect that $u-u'$, being a result of anharmonic motion, would also decrease with increasing Θ_D/T, the ratio of the Debye temperature to the temperature at which u is observed. This accounts for the zero value of $u-u'$ for NH_4F. However, in the case of AgI, Θ_D is of order 120°K, so that observable anharmonic effects are expected at room temperature. The reason that this anharmonicity is not reflected in the u parameter is clearly that for this compound motion in the four tetrahedrally oriented antibonding directions is approximately equivalent. The sign and magnitude of the difference $u-u'$ depends in a complex manner on the forces binding the atom in the solid.

Lawaetz (1972) has found an approximately linear decrease of c/a with increase in the square of the ionicity charge parameter, $ZC/\hbar\omega_p$. Here Z is the effective valence, C the Phillips electronegativity difference (Phillips, 1970) and $\hbar\omega_p$ is the plasma energy of the valence-electron gas. Lawaetz has interpreted the equilibrium of the wurtzite structure in terms of a Coulomb interaction between rigid charges $\pm Ze$ screened by an effective dielectric constant $(\hbar\omega_p/C)^2$. This Coulomb interaction thus becomes weaker as c/a increases and the wurtzite structure becomes less stable.

In Table 2 the compounds appearing highest in the table are those with the lowest c/a values. The Coulomb interaction is therefore likely to have a large influence on the preferred directions of anharmonic motion for these compounds. For compounds appearing lower in the table shorter-range forces might be expected to be of increasing importance. If the short-range repulsive core interaction was the only one to be considered, the atoms would clearly prefer to move towards the larger octahedral holes in the lattice, rather than towards the tetrahedral holes along the c axis, and the sign of $u-u'$ would be reversed. Thus it would seem that the Coulomb interaction allows preferred motion towards the tetrahedral holes, but that this effect is opposed by the short-range forces. The Coulomb interaction becomes progressively weaker as c/a increases, until for AgI the cancellation is complete.

Further insight into the nature of the u parameter is afforded by an investigation of pyroelectricity in these compounds.

Pyroelectricity in wurtzite compounds

Pyroelectric crystals are those which undergo a change in polarization, P, when subjected to a change in temperature, T. The phenomenon has been observed in several wurtzite compounds, the polarization showing a general increase in absolute value as the temperature is increased.

The pyroelectric constant has been measured in CdS, CdSe, BeO and ZnO. Grout & March (1974) have suggested that for these compounds the effect may be interpreted within the framework of the rigid-ion model. We therefore consider one of the tetrahedra of atoms that form a unit of the crystal structure. In Fig. 6(*a*) we show such a regular tetrahedron, with a cation at the centre. The c axis is directed upwards in the diagram. In this case the electric moment of the unit is exactly zero.

Since measurements of polarization are normally carried out at constant stress σ across the crystal, thermal expansion is permitted. In the above compounds the thermal expansion along the c axis is smaller than that in the $c=0$ plane. Then, if we assume that the four bonds remain equal in length, relative to one another, an increase in temperature will cause a flattening of the tetrahedron. This will produce a net electric moment directed down the c axis, as shown in an exaggerated fashion in Fig. 6(*b*). As well as distortion of the tetrahedron, the increase in temperature will cause an increase in the interatomic distances, which will contribute to the absolute value of the electric moment and correspondingly of the crystal polarization. These thermal expansion effects are known as secondary pyroelectricity, and may be subtracted from the observed value of the pyroelectric constant, $p_3^\sigma = (\mathrm{d}P/\mathrm{d}T)_\sigma$, using the equation (Nye, 1957)

$$p_3^\sigma = p_3^\varepsilon + a_j c_{jk} d_{3k} \,. \qquad (10)$$

In this equation p_3^ε is the pyroelectric constant at constant strain ε, a_j are the thermal expansion coefficients, c_{jk} are the elastic constants and d_{3k} are the piezoelectric moduli.

The remaining contribution to the observed pyroelectricity is the primary pyroelectric effect, measured by the quantity, p_3^ε. Although its origin is not well understood, for the wurtzite compounds so far investigated it is the major effect. A simple mechanism for its origin could be provided by the same type of anharmonic motion proposed as an explanation for the

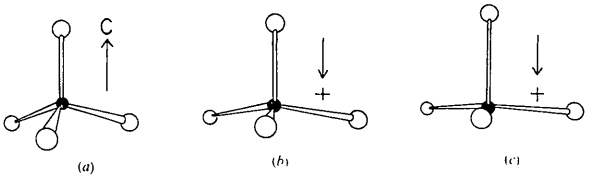

Fig. 6. (*a*) Tetrahedral unit of structure in an ideal wurtzite compound with no anharmonic effects present. (*b*) Polarized tetrahedral unit of structure after anisotropic expansion has occured with the bond lengths remaining equal to one another. (*c*) Polarized tetrahedral unit of structure showing the mean positions of the atoms if anharmonic motion towards the tetrahedral holes is preferred over that towards the octahedral holes.

observed u parameters. Under an anharmonic potential the mean positions of all the atoms are moved along the c-axis direction with respect to their equilibrium positions. However, the movement is in opposite directions for ions of opposite types, thus creating an electric moment. The situation is depicted in Fig. 6(c), where the mean positions are shown for the same sense of anharmonic motion as indicated by the observed u parameters. Fig. 6(b) may be interpreted as showing the equilibrium positions of the atoms for Fig. 6(c). The resulting contribution to the pyroelectric constant, p_3^g, is negative (we have adopted the convention that a positive pyroelectric constant results from an electric moment directed along the positive c axis).

For the wurtzite compounds where p_3^g has been measured, and for which the constants a_j, c_{jk} and d_{3k} are available, we have obtained approximate values of p_3^g, using equation (10). The accuracy of the results is limited by the lack of exact data on the parameters required and on their temperature dependence. The p_3^g are tabulated in Table 3. A comparison of this table with Table 2 shows that p_3^g and $u-u'$ are consistently of opposite sign and appear to be roughly correlated, as would be expected if both were manifestations of anharmonic motion. However, data on the pyroelectric constants of other wurtzite compounds is necessary for an adequate comparison to be made.

Bragg diffraction from wurtzite structures

Neutron and X-ray elastic scattering data from a number of cubic structures has been interpreted very successfully in terms of anharmonic one-particle potentials. In order to obtain the Bragg scattered intensity expression, we use the potential equations (1) to (4).

The attenuation of intensity of Bragg diffraction peaks due to thermal motion of the atoms in a crystal may be described in terms of a temperature factor, T_μ, for each atomic species. T_μ is the expectation value

$$T_\mu = \exp\,(i\mathbf{Q}\,.\,\mathbf{x}_\mu) \tag{11}$$

where, for elastic scattering

$$\mathbf{Q}\,.\,\mathbf{x}_\mu = 2\pi\left(\frac{hx_{1\mu}}{a}+\frac{kx_{2\mu}}{a}+\frac{lx_{3\mu}}{c}\right) \tag{12}$$

with h, k and l the three Miller indices. Following Willis (1969), we evaluate this expectation value in the classical limit. This is effectively the same as finding the Fourier transform of $\exp\,(-V_\mu/k_BT)$. We expand this quantity to obtain

$$\exp\left(\frac{-V}{k_BT}\right) = \left[1-\frac{\beta_1}{k_BT}(x_1x_2^2-x_2^2x_1) - \frac{\beta_2}{k_BT}(x_1^2-x_1x_2+x_2^2)x_3 - \frac{\beta_3}{k_BT}x_3^3\right] \times \exp\left\{\frac{-1}{k_BT}\left[V_0+\frac{\alpha_1}{2}(x_1^2-x_1x_2+x_2^2)+\frac{\alpha_3}{2}x_3^2\right]\right\} \tag{13}$$

where we have dropped the subscript μ from all parameters. This expansion limits $\exp\,(-V/k_BT)$ so that it does not diverge as the displacement becomes infinitely large, since α_1 and α_3 are positive. The atom therefore remains bounded within the solid, regardless of the signs of β_1, β_2 and β_3.

The resulting anharmonic temperature factor is then

$$T=\exp\,(-M)\left[1-i\beta_3\frac{4\pi k_BT}{\alpha_3^2}\frac{l}{c}\left(\tfrac{3}{2}-\frac{2\pi^2k_BT}{\alpha_3}\frac{l^2}{c^2}\right) - i\beta_2\tfrac{16}{3}\frac{\pi k_BT}{\alpha_1\alpha_3}\frac{l}{c}\left(\tfrac{3}{4}-\frac{2\pi^2k_BT}{\alpha_1}\frac{(h^2+hk+k^2)}{a^2}\right) - i\beta_1\tfrac{128}{9}\frac{\pi^3(k_BT)^2}{\alpha_1^3a^3}\left(\frac{h^3-k^3}{3}+\frac{h^2k-hk^2}{2}\right)\right] \tag{14}$$

where terms of order β_i^2 and higher have been omitted. In this expression, $\exp\,(-M)$ is the harmonic temperature factor:

$$M=\frac{8\pi^2k_BT}{3\alpha_1}\frac{(h^2+hk+k^2)}{a^2}+\frac{2\pi^2k_BT}{\alpha_3}\frac{l^2}{c^2} = \frac{(h^2+hk+k^2)}{3a^2}B_{11}+\frac{l^2}{4c^2}B_{33} \tag{15}$$

where

$$B_{11}=\frac{8\pi^2k_BT}{\alpha_1} \tag{16}$$

and

$$B_{33}=\frac{8\pi^2k_BT}{\alpha_3} \tag{17}$$

are the conventional Debye–Waller factors.

To obtain the expression for the Bragg intensities we use the generalized structure-factor formalism of Dawson (1967). We write for the X-ray atomic scattering factor

$$f_{0\mu}=f_\mu+if_\mu'' \,. \tag{18}$$

Here f_μ includes the real part of the dispersion correction and f_μ'' is the imaginary part of the dispersion

Table 3. *Values for the primary pyro-electric constant*

Compound	$p_3^g\times10^{-10}$ (C/cm² °K) (averaged over temperature range 77 to 298 °K)	Reference
ZnO	$-5(\pm1)$	Heiland & Ibach (1966)
BeO	$-3{\cdot}4$	Smith, Newkirk & Kahn (1964)
CdS	$-3{\cdot}1$	Berlincourt, Jaffe & Shiozawa (1963)
CdSe	$-2{\cdot}9$	Berlincourt, Jaffe & Shiozawa (1963)

correction. The temperature factor is similarly divided into real and imaginary parts

$$T_\mu = t_\mu + i\tau_\mu , \tag{19}$$

the real part being in this case purely harmonic. The structure factor is then:

$$F = \sum_\mu f_{0\mu} T_\mu \exp(2\pi i \mathbf{Q} \cdot \mathbf{x}_{0\mu}) \tag{20}$$

where $\mathbf{x}_{0\mu}$ are the rest positions of the four atoms defining the unit cell. It is clear from Fig. 1 that the asymmetric unit contains four atoms, two of them of type A and two of type B. Furthermore, each atomic type occupies one of two non-equivalent lattice sites, which we shall label A, A′ and B, B′ respectively. The two types of site are related to each other by a rotation of π about the c axis. Thus the parameter β_1 is of opposite sign for the atoms on the A (or B) sites compared to those on the A′ (or B′) sites, but the parameters β_2 and β_3 are invariant to these changes of site. So that the intensity may be represented purely in terms of parameters for atoms on the unprimed sites, it is convenient to divide the imaginary part of the temperature factor, τ_μ, into two parts

$$\tau_\mu = t'_\mu + t''_\mu \tag{21}$$

where t'_μ contains the term with coefficient β_1 in equation (14) and t''_μ contains those with coefficients β_2 and β_3. Then we obtain for the kinematic intensity, $I = F^*F$

$$\begin{aligned} I = 2\left[1+(-1)^l \cos 2\pi\frac{(h+2k)}{3}\right]\{&f_A^2 t_A^2 + f_B^2 t_B^2 \\ &+ 2\cos(2\pi l u') f_A f_B t_A t_B + 2\sin(2\pi l u')[(f''_A f_B \\ &- f_A f''_B) t_A t_B + f_A f_B (t''_A t_B - t_A t''_B)]\} \\ &+ 4(-1)^l \sin\frac{(h+2k)}{3}\{f_A^2 t_A t'_A \\ &+ f_B^2 t_B t'_B + f_A f_B (t_A t'_B + t'_A t_B)\cos(2\pi l u')\} \end{aligned} \tag{22}$$

where terms of order $f''t'$, $f''t''$, f''^2, t''^2 and t'^2 have been ignored.

We see that equation (22) includes all the usual terms obtained in the harmonic approximation as well as additional anharmonic terms involving t' and t''. The equation is applicable for neutrons if f_μ is replaced by the scattering length; dispersion effects with neutrons are in general negligible, so f''_μ is then zero.

Inspection of equations (14) and (22) shows that harmonically equivalent reflexions need no longer be equivalent in the anharmonic treatment, because of the additional anisotropy introduced. This is, of course, analogous to the anisotropic effect previously obtained for cubic crystals under an anharmonic treatment (Willis, 1969).

Further insight into the anharmonic term in equation (22) may be obtained by expressing the quantity $(u-u')$ in terms of the coefficients of the one-particle potential. $(u-u')$ is in fact just the difference in the expectation value of x_3 for the two types of atom. Thus:

$$\begin{aligned} (u-u') &= \frac{1}{c}(\langle x_{3B}\rangle - \langle x_{3A}\rangle) \\ &= \frac{kT}{c}\left[3\left(\frac{|\beta_{3B}|}{\alpha_{3B}^2} + \frac{|\beta_{3A}|}{\alpha_{3A}^2}\right) - 2\left(\frac{|\beta_{2B}|}{\alpha_{1B}\alpha_{3A}} + \frac{|\beta_{2A}|}{\alpha_{1A}\alpha_{3A}}\right)\right]. \end{aligned} \tag{23}$$

Equation (23) is closely related to the first-order anharmonic terms of equation (14). If t''_μ of equation (21) includes only these first-order terms we may write:

$$(t''_A t_B - t_A t''_B) = -t_A t_B 2\pi l (u-u') . \tag{24}$$

Thus if $\cos(2\pi l u)$ is used in equation (21) instead of $\cos(2\pi l u')$, then the anharmonic effects are already included to first order, since

$$\begin{aligned} t_A t_B \cos(2\pi l u) \approx\ & t_A t_B \cos(2\pi l u') \\ & + (t''_A t_B - t_A t''_B)\sin(2\pi l u') \end{aligned} \tag{25}$$

for $(u-u') \ll u$.

However the higher-order anharmonic effects described by the terms containing t'_μ in equation (22) are not accounted for by this approximation. Terms of similar order in t''_μ are also ignored in equation (24). Thus to interpret successfully accurate intensity data from wurtzite crystals the full anharmonic treatment may be required.

We note that equation (22) for the intensity of elastic scattering would be complicated in the case of X-rays if the effects of bonding were included in the scattering factors. However, these effects are only observable at low angles where anharmonic effects are minimal. Further consideration of this problem is outside the scope of this paper.

Discussion

There is good reason to suppose that anharmonic motion in the four antibonding directions of a wurtzite structure has been observed as long ago as 1935 (Helmholz, 1935). Oscillation data collected at room temperature from the cleavage face of a single crystal of AgI, using Mo $K\alpha$ radiation, approximately fitted an ideal wurtzite structure. However, a careful analysis showed that a more satisfactory model allowed each silver atom to occupy randomly four positions slightly displaced in the antibonding directions from the ideal position. Anharmonic motion of the silver atom provides a physically more acceptable explanation, especially since the data collected from the crystal at liquid-air temperatures very nearly fitted the ideal wurtzite structure.

Burley (1963), in a more recent study of AgI using precession data, has observed a charge depletion in the bonding directions, as shown by a difference Fourier projection along the c axis. This is in support of the observations of Helmholz and is further evidence of anharmonic motion along the antibonding directions. It is not recognized as such by Burley, as a result apparently of a misinterpretation of Helmholz's work.

An effect similar to that observed in AgI at room temperature was noticed by Hoshino (1952) in powder photographs at 430 °C of the wurtzite phase of CuBr. An analogous effect occurred for the zincblende phase of the same powder observed at room temperature. Interpretation of both effects as anharmonic thermal vibration would again appear to provide a better approximation to the true situation. This was, in fact, recognized by Miyake & Hoshino (1958) in a review of the work. Further experimental study of these halides would evidently provide valuable quantitative results for the cubic anharmonic parameters introduced in the early part of this paper.

We wish to thank Mr Grant Moss for valuable discussions. S. Mair gratefully acknowledges the financial support of a Commonwealth Postgraduate Research Award.

References

ADRIAN, H. W. W. & FEIL, D. (1969). *Acta Cryst.* A**25**, 438–444.
BARNEA, Z. (1973). Ph. D. Thesis, Univ. of Melbourne.
BERLINCOURT, D., JAFFE, H. & SHIOZAWA, L. R. (1963). *Phys. Rev.* **129**, 1009–1017.
BURLEY, G. (1963). *J. Chem. Phys.* **38**, 2807–2812.
COOPER, M. J., ROUSE, K. D. & FUESS, H. (1973). *Acta Cryst.* A**29**, 49–56.
DAWSON, B. (1967). *Proc. Roy. Soc.* A**298**, 255–263.
DAWSON, B. & WILLIS, B. T. M. (1967). *Proc. Roy. Soc.* A**298**, 307–315.
GROUT, P. J. & MARCH, N. H. (1974). *Phys. Lett.* **47**A, 288–290.
HEILAND, G. & IBACH, H. (1966). *Sol. State Commun.* **4**, 353–356.
HELMHOLZ, L. (1935). *J. Chem. Phys.* **3**, 740–747.
HOSHINO, S. (1952). *J. Phys. Soc. Japan*, **7**, 560–571.
JEFFREY, G. A., PARRY, G. S. & MOZZI, R. L. (1956). *J. Chem. Phys.* **25**, 1024–1031.
KEFFER, F. & PORTIS, A. M. (1957). *J. Chem. Phys.* **27**, 675–682.
LAWAETZ, P. (1972). *Phys. Rev.* B**5**, 4039–4045.
MIYAKE, S. & HOSHINO, S. (1958). *Rev. Mod. Phys.* **30**, 172–174.
NYE, J. F. (1957). *Physical Properties of Crystals*, p. 187. Oxford: Clarendon Press.
PHILLIPS, J. C. (1970). *Rev. Mod. Phys.* **42**, 317–356.
PRYOR, A. W. & SABINE, T. M. (1964). *J. Nucl. Mater.* **14**, 275–281.
SABINE, T. M. & HOGG, S. (1969). *Acta Cryst.* B**25**, 2254–2256.
SMITH, D. K., NEWKIRK, H. W. & KAHN, J. S. (1964). *J. Electrochem. Soc.* **111**, 78–87.
WILLIS, B. T. M. (1969). *Acta Cryst.* A**25**, 277–300.

Acta Cryst.(1975). A**31**, 207

Thermoelastic Properties of Potassium Hydrogen Sulphate

BY D. GERLICH*† AND H. SIEGERT

Institut für Kristallographie, Universität zu Köln, D-5000 Köln 41, Germany (BRD)

(*Received* 16 *September* 1974; *accepted* 7 *October* 1974)

The room-temperature elastic moduli, their temperature derivatives and the thermal expansion of $KHSO_4$ have been measured. Both the elastic and the thermal properties exhibit a quasi-hexagonal symmetry, the crystalline *a* axis being the unique axis. On the other hand, the Grüneisen tensor is essentially isotropic. A qualitative correlation of these phenomena with the crystal structure is made.

Introduction

The family of the hydrogen sulphate salts form an interesting group of materials, as the binding in the crystal is characterized by the presence of strong hydrogen bonds. These bonds are also responsible for the ferroelectric phase transitions found in ammonium and rubidium hydrogen sulphates, (Pepinsky, Vedam, Hoshino & Okaya, 1958; Pepinsky & Vedam, 1960). Although the ferroelectric phase transition in the latter materials has been investigated extensively, no elastic data are available for any material in the above group. Thus, an investigation of the thermoelastic properties of potassium hydrogen sulphate, $KHSO_4$, as the first of the HSO_4 group, was undertaken. In addition to the existence of hydrogen bonds (Loopstra & MacGillavry, 1958), the material is known to have several phase transitions (Bridgman, 1916/1917). It should therefore be of interest to measure its thermoelastic properties, to try to correlate the latter with the direction and strength of the existing hydrogen bonds, and to see whether any indication of the occurrence of

* Supported by Deutscher Akademischer Austauschdienst.
† Permanent address: Department of Physics & Astronomy, Tel Aviv University, Ramat Aviv, Israel.